Russell and M. G. Tomasko (*Origins Life*, in press).
3. J. L. Weinberg, M. S. Hanner, D. E. Beeson, L. M. DeShields II, B. A. Green, *J. Geophys. Res.* **79**, 3665 (1974).
4. M. S. Hanner, J. L. Weinberg, L. M. DeShields II, B. A. Green, G. N. Toller, *ibid.*, p. 3671.
5. D. L. Coffeen, *ibid.*, p. 3645.
6. M. G. Tomasko, A. E. Clements, N. D. Castillo, *ibid.*, p. 3653.
7. W. Swindell and L. R. Doose, *ibid.*, p. 3634.
8. T. Gehrels, in *Planetary Satellites*, J. A. Burns, Ed. (Cornell Univ. Press, Ithaca, New York, in press).
9. J. W. Fountain, D. L. Coffeen, L. R. Doose, T. Gehrels, W. Swindell, M. G. Tomasko, *Science* **184**, 1279 (1974); T. Gehrels, *J. Geophys. Res.* **79**, 4305 (1974).
10. T. C. Duxbury, *Bull. Am. Astron. Soc.*, in press.
11. B. A. Smith, personal communication.
12. M. G. Tomasko, *Bull. Am. Astron. Soc.*, in press.
13. A. B. Binder and D. W. McCarthy, *Astron. J.* **78**, 939 (1973).
14. C. B. Pilcher and T. B. McCord, *Astrophys. J.* **165**, 195 (1971).
15. R. E. Danielson and M. G. Tomasko, *J. Atmos. Sci.* **26**, 889 (1969).
16. L. Axel, *Astrophys. J.* **173**, 451 (1972).
17. J. T. Bergstralh, *Icarus* **19**, 390 (1973).
18. L. M. Trafton and P. H. Stone, *Astrophys. J.* **188**, 649 (1974).
19. T. Gehrels, B. Herman, T. Owen, *Astron. J.* **74**, 190 (1969); a further discussion by T. Gehrels is presented in *Origins Life*, in press.
20. A. E. Clements, thesis, University of Arizona (1974).
21. We thank B. A. Smith for his comments on this paper and M. E. Arthur, G. A. Kew, and J. Golson for their help, especially during the encounter operations. We were able to optimize the performance of our instrument, thanks to the special support we received from the personnel of the Pioneer Project Office, the Bendix Corporation, and NASA's Deep Space Network. Our work is supported by the Pioneer Project Office at NASA Ames Research Center.

14 March 1975

Pioneer 11 Infrared Radiometer Experiment: The Global Heat Balance of Jupiter

Abstract. *Data obtained by the infrared radiometers on the Pioneer 10 and Pioneer 11 spacecraft, over a large range of emission angles, have indicated an effective temperature for Jupiter of 125° ± 3°K. The implied ratio of planetary thermal emission to solar energy absorbed is 1.9 ± 0.2, a value not significantly different from the earth-based estimate of 2.5 ± 0.5.*

Data from the Pioneer 10 and Pioneer 11 infrared radiometers provide a good sample of the infrared emission of Jupiter as a function of latitude and emission angle. Pioneer 10 gave one map in each of two broad spectral channels, each map consisting of an image centered at 11°S on Jupiter (*1*). Pioneer 11 gave two maps in each channel, an inbound map centered at 41°S and a partial outbound map centered at 52°N. About one-half of the outbound viewing period was lost as a result of false commands during passage through the radiation belts. The spatial resolution on Jupiter ranged from 1/30 to 1/200 of the planetary diameter. More than ¾ of the surface area of Jupiter was viewed by the radiometers.

The absolute calibration, with respect to a blackbody, was done in the laboratory before the flight. In-flight calibration, relative to the laboratory value, is provided by a calibrator plate at a known temperature which is moved into the field of view once every 12 seconds (*2*). The zero is set when looking at space, and the response to the calibrator plate is then compared with the response measured in the laboratory. No significant changes occurred during the flight. Both before and after encounter on Pioneer 10 and Pioneer 11 the response in each channel differed from the laboratory value by no more than 3 percent. Our estimates of the uncertainty arising from the calibration procedures range from ±4 to ±8 percent. The latter value will be used throughout this report.

The two spectral channels are centered at wavelengths λ of 20.0 and $\lambda =$ 45.4 μm and have equivalent widths of 11.6 and 22.7 μm, respectively. The measured intensities I_λ are fitted to low-order polynomials in μ and μ_l, where $\mu = \cos\theta$ is the cosine of the emission angle and $\mu_l = \sin l$ is the sine of the latitude. The flux versus latitude $[F_\lambda(\mu_l)]$ and the globally averaged flux $(\overline{F}_\lambda)$ in each channel are then derived from the formulas

$$F_\lambda(\mu_l) = 2\pi \int_0^1 \mu I_\lambda(\mu, \mu_l)\, d\mu$$

and

$$\overline{F}_\lambda = \frac{1}{2}\int_{-1}^{1} \frac{(1 - 2\epsilon\mu_l^2)F_\lambda(\mu_l)\, d\mu_l}{(1 - 2\epsilon/3)}$$

where ε is the oblateness of Jupiter, approximately equal to 0.065 (*3*). Terms of order ε^2 have been neglected.

The values of $F_\lambda(\mu_l)$ and $\overline{F}_\lambda$ depend on the method one employs to average the data, for example, using second-order instead of third-order polynomials, folding the northern and southern hemisphere data together instead of treating them separately, or using Pioneer 10 and Pioneer 11 data combined instead of treating them separately. The spread of values provides an estimate of additional uncertainties that are not included in the ±8 percent associated with the absolute calibration. These additional uncertainties appear to be small. Estimates of $\overline{F}_\lambda$ obtained from Pioneer 10 and Pioneer 11 data treated separately differ from those obtained from the combined data by no more than 3 percent. Different polynomial fits to the combined data give values of $\overline{F}_\lambda$ differing by no more than 1 percent. In addition, the values of $F_\lambda(\mu_l)$ appear to be very nearly independent of latitude, $F_{20}(\mu_l)$ decreasing and $F_{45}(\mu_l)$ increasing from the equator to the pole by about 5 percent, respectively. The values of $\overline{F}_{20}$ and $\overline{F}_{45}$ obtained in this way are 3035 and 5100 erg cm^{-2} sec^{-1}, respectively.

The sum $(\overline{F}_{20} + \overline{F}_{45})$ represents a significant fraction of the average emitted flux $F = \sigma T_e^4$ integrated with respect to wavelength, where σ is the Stefan-Boltzmann constant. The precise value of this fraction depends on the planetary emission in spectral ranges outside the two channels as shown in Table 1. If the planetary emission were to follow a blackbody spectrum, then $F/(F_{20} + F_{45}) = 1.725$. Radiative-convective equilibrium models (*4*), in which the effective temperature T_e and the ratio of He to H_2 are free parameters, give $F/(F_{20} + F_{45}) = 1.723$. Finally, by direct inversion of the intensity data, in which the vertical thermal structure is adjusted so that $I_{20}(\mu)$ and $I_{45}(\mu)$ agree with ob-

Table 1. Estimates of the ratio of the total emitted flux $F = \sigma T_e^4$, integrated with respect to wavelength, to the sum of the fluxes $F_{20} + F_{45}$ observed in the spectral channels of the radiometer.

Description of model	Ratio
Blackbody	
$T_e = 120°K$	1.752
$T_e = 130°K$	1.700
Best fit to $F_{20} + F_{45}$	1.725
Radiative equilbrium (*4*)	
$T_e = 123.8°K$, $He/H_2 = 1.0$	1.736
$T_e = 131.5°K$, $He/H_2 = 1.0$	1.673
$T_e = 124.9°K$, $He/H_2 = 0.0$	1.704
Best fit to $F_{20} + F_{45}$, F_{45}/F_{20}	1.723
Direct thermal inversion (*5*)	
$T_e = 127.9°K$ (SEB)	1.694
$T_e = 124.6°K$ (STrZ)	1.730
Adopted value (this study)	
$T_e = 125° \pm 3°K$	1.72 ± 0.03

servation, one obtains $F/F_{20}+F_{45}) =$ 1.694 and 1.730 in the South Equatorial Belt (SEB) and South Tropical Zone (STrZ) respectively (*5*).

All these models have a brightness temperature which remains constant to within ±20°K with respect to wavelength. This is consistent with ground-based observations in the range from 8 to 14 μm (*6*) and in the range from 1 to 2 cm (*7*). Accordingly, we have adopted the value 1.72 ± 0.03. With the observed values of $\overline{F}_{20}$ and $\overline{F}_{45}$, this gives an effective temperature T_e for Jupiter of 125° ± 3°K, where the uncertainty is almost entirely in the calibration.

The ratio of total emitted power E to absorbed solar power S for Jupiter is given by

$$\frac{E}{S} = \frac{4\sigma T_e^4(1 - 2\epsilon/3)}{(1 - A)F_s(1 - \epsilon)} \approx 1.9$$

Here F_s is the solar flux at Jupiter's orbit, and $A = 0.42$ is the bolometric Bond albedo (*8*). The uncertainty in $(1-A)$ is at least as great as that associated with σT_e^4. Our measurements thus are not inconsistent with the value $E/S = 2.5 \pm 0.5$, previously determined by earth-based observations (*9*).

Future papers will deal with the basic data related to the global heat balance, the implications of our measurements on the vertical thermal structure of Jupiter's atmosphere, and the heat balance of local regions on the planet. Preliminary results (*5*) of these studies reveal, first, that temperatures and pressures agree with ground-based values (*4, 7, 10*) but do not agree with the Pioneer 10 radio occultation results (*11*), and, second, that the molar fraction of He is not greater than 0.4. As previously remarked (*1*), the measured temperature field is incompatible with model calculations for an atmosphere in radiative-convective equilibrium, so such calculations cannot be used as originally planned (*12*) to obtain a more accurate estimate of the He abundance.

A. P. INGERSOLL, G. MÜNCH
G. NEUGEBAUER, D. J. DINER
G. S. ORTON, B. SCHUPLER
M. SCHROEDER
California Institute of Technology, Pasadena 91125
S. C. CHASE, R. D. RUIZ
Santa Barbara Research Center, Santa Barbara, California
L. M. TRAFTON
University of Texas, Austin 78712

References and Notes

1. S. C. Chase, R. D. Ruiz, G. Münch, G. Neugebauer, M. Schroeder, L. M. Trafton, *Science* **183**, 315 (1974).
2. M. L. Bender *et al.*, *Appl. Opt.* **13**, 2623 (1974).
3. J. D. Anderson, G. W. Null, S. K. Wong, *Science* **183**, 322 (1974).

L. M. Trafton, *Astrophys. J.* **147**, 765 (1967); ——— ; G. Münch, *J. Atmos. Sci.* **26**, 813 (196 L. M. Trafton, *Astrophys. J.* **179**, 971 (1973).

5. G. S. Orton, thesis, California Institute of Technology (1975).

F. C. Gillett, F. J. Low, W. A. Stein, *Astrophys. J.* **157**, 925 (196 D. K. Aitken and B. Jones, *Nature (Lond.)* **240**, 230 (1972).

S. Gulkis and R. Poynter, *Phys. Earth Planet. Interiors* **6**, 36 (1972).

D. J. Taylor, *Icarus* **4**, 362 (1965); M. G. Tomasko, A. E. Clements, N. D. Castillo, *J. Geophys. Res.* **79**, 3653 (1974).

H. H. Aumann, C. M. Gillespie, Jr., F. J. Low, *Astrophys. J.* **157**, L69 (196 K. R. Armstrong, D. A. Harper, Jr., F. J. Low, *ibid.* **178**, L89 (1972).

L. Wallace, M. Prather, M. J. S. Belton, *Astrophys. J.* **193**, 481 (1974).

11. A. Kliore, D. L. Cain, G. Fjeldbo, B. L. Seidel, S. I. Rasool, *Science* **183**, 323 (1974).

D. M. Hunten and G. Münch, *Space Sci. Rev.* **14**, 433 (1973).

13. We thank J. Bennett for her efforts in the programming and data reduction. The cooperation of all the personnel of the Pioneer Project is gratefully acknowledged.

14 March 1975

Pioneer 11 Meteoroid Detection Experiment: Preliminary Results

Abstract. *The concentration of meteoroids of mass ~ 10^{-8} gram in interplanetary space, in the asteroid belt, and near Jupiter has been measured. The data confirm the Pioneer 10 observation that the asteroid belt is not highly populated with small meteoroids, suggest that the high concentration of small particles around Jupiter is the result of gravitational focusing, and provide an indication of the mass distribution of meteoroids in interplanetary space.*

The first measurements of the population of small meteoroids outside the orbit of Mars were made with the meteoroid detection experiment on Pioneer 10 (*1*). The Pioneer 10 detector was sensitive to particles of mass ~ 10^{-9} g. A similar experiment on Pioneer 11, sensitive to particles of mass ~ 10^{-8} g, has now provided us with data on the mass distribution of meteoroids in interplanetary space. The meteoroid detectors on Pioneer 11 are pressurized cell penetration detectors like those on Pioneer 10 except that the cell wall exposed to the meteoroid environment is 50 μm thick, twice as thick as those on Pioneer 10 (*2*). There are 234 pressurized cells on each spacecraft, divided into two data channels to increase reliability. The data from 108 cells are processed by the channel 0 instrument, whereas the data from the other 126 cells are processed by the channel 1 instrument.

The time history of the meteoroid penetrations on the channel 0 instrument is shown in Fig. 1. The Pioneer 10 data are also shown for comparison. The approximate heliocentric range is indicated on the upper scale.

On Pioneer 11 the penetration rate was high between 1.00 and 1.15 astronomical units (A.U.). There were no meteoroid penetrations between 1.15 and 2.3 A.U. The penetration rate between 2.3 and 5.0 A.U. was lower than that measured between 1.00 and 1.15 A.U. There was no increase in the penetration rate in the asteroid belt and hence no evidence that the asteroid belt is a significant source of small meteoroids.

The Pioneer 11 data can be compared directly with the Pioneer 10 data for interplanetary space because the interplanetary trajectories were similar. The penetration rates differed by about a factor of 2 near 1 A.U., in agreement

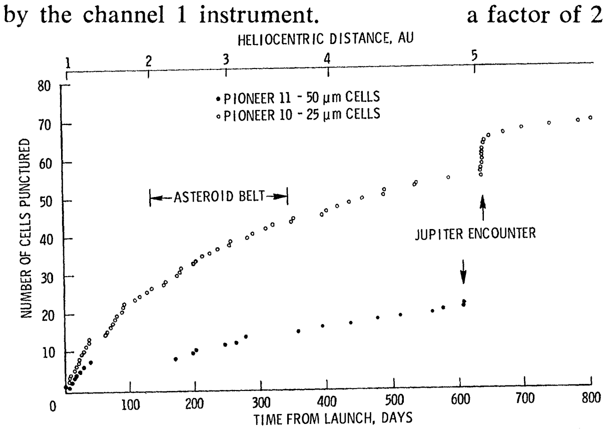

Fig. 1. Time history of meteoroid penetrations detected on the Pioneer 11 channel 0 instrument. Pioneer 10 data are shown for comparison.